Supplemental Information

Michael W. Martinez-Szewczyk, Steven DiGregorio, Owen Hildreth, Mariana I. Bertoni,
"Reactive Silver Inks: A Path to Solar Cells with 82% less Silver".

1. RSI Printing Parameters

Samples for the top-down microscopy were printed with 4.5 µg/cm and samples for cross-section microscopy were printed with 18 µg/cm. Because the different inks contained different silver concentrations, the printing parameters were adjusted accordingly to obtain an identical silver amount between the two ink systems. The flow rate was kept constant at 1 µl/min for the top-down samples and 2 µl/min for the cross-section samples. From there, the printing speed and number of layers printed were adjusted, which can be seen below in Table S1, to achieve an identical silver amount. Fig. S1 shows a picture of the printing setup.

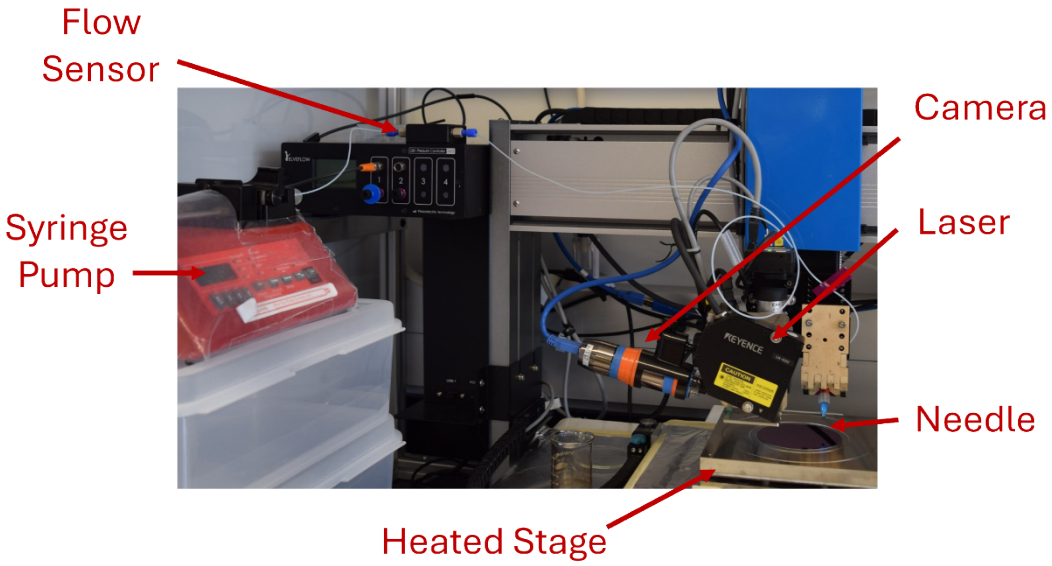

Figure S1:Picture of RSI printing setup

Table S1: Printing parameters for the top-down and cross-section samples

Ink Type	Top-Down Samples		Cross-Section Samples	
	Printing Speed (mm/s)	# of Layers	Printing Speed (mm/s)	# of Layers
Ethylamine 0.5 M	10	5	25	25
Ammonia 2.2 M	17.5	2	50	11

2. Needle Printing Pressure
   In order to calculate the pressure applied by the needle on the substrate during printing one can use the vertical needle deflection of ~ 50 µm. Using this along with the needle angle (45°), material (fused quartz with polyimide coating), and needle geometry (10mm shaft length, 90 µm outer diameter, 20 µm inner diameter) the downward force can be calculated.

3. Line Resistivity Details
   The line resistance of RSI was measured on ITO to represent the solar cell substrate and is shown below in Fig. S2. Sputtered Ag pads were used to probe the RSI line without probe tip damage. The resistance of the sputtered pad was reliably at least two orders of magnitude higher than the ITO and as a result had very little impact on the measurement of the RSI by the parallel resistors formula[1] given below.

$$\frac{1}{R_{measured}} = \frac{1}{R_{silver}} + \frac{1}{R_{ITO}}$$

$$\frac{1}{R_{silver}} = \frac{1}{R_{measured}} - \frac{1}{R_{ITO}}$$

$$R_{silver} = \frac{1}{\frac{1}{R_{measured}} - \frac{1}{R_{ITO}}}$$

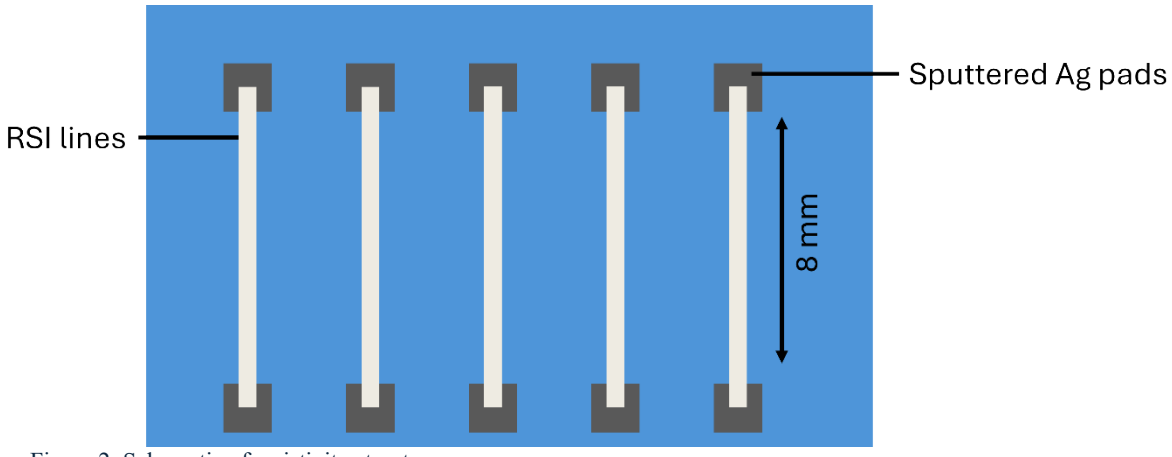

Figure 2: Schematic of resistivity structure.

4. TLM Contact Resistance Details

The contact resistance of the ITO/RSI finger was measured using the transfer length method (TLM). Fig. S3 shows a schematic of the TLM structure used in the above work. The distances chosen for S1-4 were 0.7, 1, 1.5, and 2.75 mm respectively. As stated above in the text, the sputtered Ag pads are used to probe the electrical performance of the printed RSI lines without the risk of damaging the lines with the probe tips.

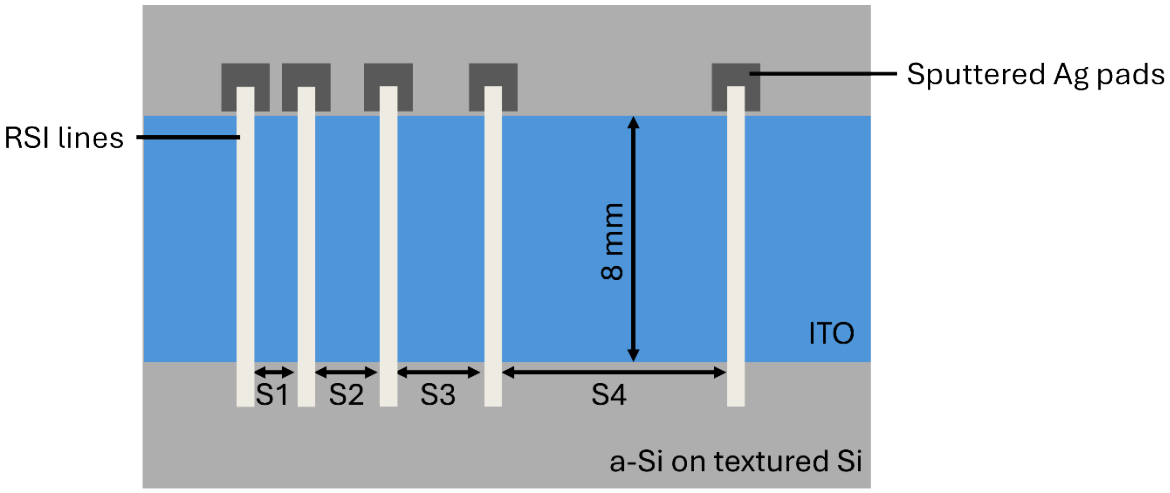

Figure S3: Schematic of TLM structure

5. SunSolve and Quokka 3 Modeling

The optical properties of the devices were simulated with the ray-tracing package SunSolve and the electrical properties were simulated with the Quokka 3 software. First, the optical performance was used to match experimental reflectance data. The calculated current generation profiles from SunSolve were then input into Quokka 3. Listed below in Table S2 are the input parameters for the SunSolve and Quokka 3 modelling.

Table S2: Modelling Input Parameters		
SunSolve	Wafer thickness (μm)	150
	Cell size (mm)	156.75
	Cell area (cm^2)	244.315
	Solar spectrum	AM 1.5G
	Zenith (°)	0
	Azimuth (°)	0
Quokka 3	Grid pitch (mm)	2.21
	R_{shunt} (Ω)	550
	RSI ρ (μΩ•cm)	3.1
	LT-SP ρ (μΩ•cm)	20
	RSI ρ_c (mΩ•cm^2)	3.13
	LT-SP ρ_c (mΩ•cm^2)	10
	Wafer resistivity (Ω•cm)	1.1
	J_0 (fA/cm^2)	2.38
	Ideality factor	1.29
	Bulk lifetime @ 10^{15} cm^{-3}(ms)	2.13

6. Griddler Power Loss Calculations

Griddler 2.5 is a 2-D finite element method (FEM) that can be used to model the performance of a solar cell with arbitrary metallization geometries[2].The cell plane is meshed into triangular elements and corresponding nodes. It then calculates the voltage at the nodes for front and rear planes of the cell based on the photocurrent received by each node. The current density perpendicular to the solution plane at each node is given by the following equations:

$$J = J_{sc}(x,y) - J_R(V(x,y))$$

$$J_R(V(x,y)) = J_{01,node}\left[\exp\left(\frac{qV(x,y)}{kT}\right) - 1\right] + J_{02,node}\left[\exp\left(\frac{qV(x,y)}{2kT}\right) - 1\right]$$

The FEM is typically more accurate than simple ohmic power loss calculations due to lateral current flow within the planes. This is because the underlying assumptions for the simple power loss equations are 1) each node acts as a current source and has the same current density and 2) that current flows perpendicular to the nearest finger and then parallel along the finger until it reaches the busbar. Both of these assumptions break down once the voltage has surpassed the maximum power point of the device.

The optical loss of current density in the presence of free carrier absorption (FCA) is given below by the equations:

$$J_{loss,FCA} = q\int_0^\infty (A_{Si,no\ FCA}(\lambda) - A_{Si,with\ FCA}(\lambda))\Phi(\lambda)d\lambda$$

Where q is the elementary charge, λ is the wavelength, $\Phi(\lambda)$ is the photon flux per unit wavelength ($cm^{-2}s^{-2}nm^{-1}$), $A_{si,no\ FCA}(\lambda)$ is the spectral absorptance in the active area without FCA, and $A_{si,with\ FCA}(\lambda)$ is the spectral absorptance with FCA.

$$A_{Si,no\ FCA}(\lambda) = T\frac{(1-T_1)+T_1R_{b1}(1-T_2)+T_1T_2R_{b1}R_{f1}(1-T_n)(1+R_{bn}T_{n)}}{1-R_{bn}R_{fn}T_n^2}$$

Where T is the transmittance, and the rest of the parameters are light trapping parameters from Basore [3].

$$A_{Si,with\ FCA}(\lambda) = TT_0\frac{\alpha_{BB}(\lambda)}{\alpha_{FCA}(\lambda,z)+\alpha_{BB}(\lambda)}\frac{\left(1-T_1^{'}\right)+T_1^{'}R_{b1}^{'}\left(1-T_2^{'}\right)+T_1^{'}T_2^{'}R_{b1}^{'}R_{f1}^{'}(1-T}{1-R_{bn}^{'}R_{fn}^{'}T_n^{'2}}$$

Where T_0 is the transmittance after accounting for FCA, α_{BB} is the band to band absorption coefficient [4], α_{FCA} is the free carrier absorption coefficient from [5], and the T_1', T_2', T_n', R_{n1}', R_{fn}', R_{b1}', R_{bn}' terms are similar to the unprimed terms but with the FCA in the wafer bulk taken into account.

The Griddler 2.5 software was used to calculate the power loss for the devices modeled previously with SunSolve and Quokka 3. The resulting power losses for RSI-metallized cells can be seen in the main text in Fig.6. Fig. S3 shows the power loss for the created model in Griddler 2.5 compared to the power losses calculated by Leilaeioun et al.[6]. This agreement between the two are within 1.1% and served as the basis for further TCO optimization while using RSI metallization.

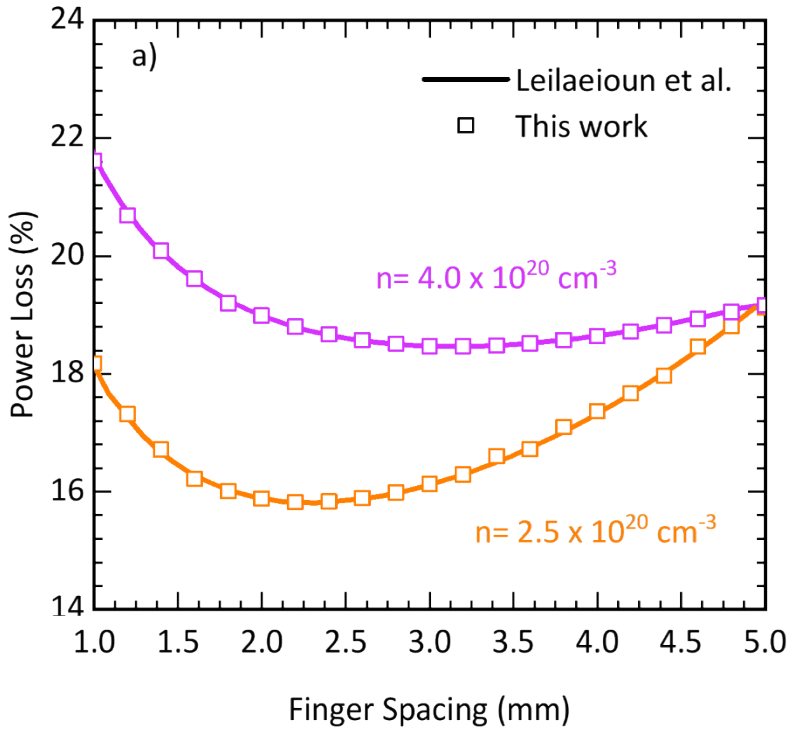

Figure S4: Calculated power loss curves for a) various TCO carrier concentrations using Griddler 2.5 (markers) vs the power loss curves calculated in Leilaeioun et al.(solid lines). The calculated power losses are within ±1.1% from literature values indicating the accuracy of the constructed model.

References

[1] C. Hooge, '21.1 Resistors in Series and Parallel', *BCIT Physics 0312 Textbook*, 2016.

[2] J. Wong, 'Griddler: Intelligent computer aided design of complex solar cell metallization patterns', in *Proc. IEEE 39th Photovolt. Specialists Conf. (PVSC)*, Jun. 2013, pp. 933–938.

[3] P. A. Basore, 'Extended spectral analysis of internal quantum efficiency', in *Conference Record of the Twenty Third IEEE Photovoltaic Specialists Conference-1993 (Cat. No. 93CH3283-9)*, 1993, pp. 147–152.

[4] M. A. Green, 'Self-consistent optical parameters of intrinsic silicon at 300 K including temperature coefficients', *Solar Energy Materials and Solar Cells*, vol. 92, no. 11, pp. 1305–1310, 2008.

[5] K. R. McIntosh, D. Yan, K. C. Fong, and T. C. Kho, 'Near-infrared free carrier absorption in heavily doped silicon', *J Appl Phys*, vol. 116, no. 6, 2014.

[6] M. A. Leilaeioun *et al.*, 'Power Losses in the Front Transparent Conductive Oxide Layer of Silicon Heterojunction Solar Cells: Design Guide for Single-Junction and Four-Terminal Tandem Applications', *IEEE J Photovolt*, vol. 10, no. 2, pp. 326–334, Mar. 2020, doi: 10.1109/JPHOTOV.2019.2954765.